Journal of Statistical Physics
https://doi.org/10.1007/s10955-019-02454-6

Finger Growth and Selection in a Poisson Field

N. R. McDonald[1]

Received: 18 July 2019 / Accepted: 22 November 2019

Abstract
Solutions are found for the growth of infinitesimally thin, two-dimensional fingers governed by Poisson's equation in a long strip. The analytical results determine the asymptotic paths selected by the fingers which compare well with the recent numerical results of Cohen and Rothman (J Stat Phys 167:703–712, 2017) for the case of two and three fingers. The generalisation of the method to an arbitrary number of fingers is presented and further results for four finger evolution given. The relation to the analogous problem of finger growth in a Laplacian field is also discussed.

Keywords Poisson paths · Laplacian growth · Free boundary problems · Conformal mapping

1 Introduction

Systems in which an interface separating two different phases evolving in response to diffusion arise in many different scenarios over widely varying scales. Even in two dimensions the deforming interface frequently leads to complicated, often striking, patterns. Examples include Saffman–Taylor fingering [16], diffusion limited aggregation [18], the formation of ramified river valley networks by groundwater flow [6,15], combustion fronts [19], magnetic flux dendrite formation in superconductors [10], and growth of bacterial colonies [8]. In all these examples the interface is characterised by long narrow protrusions—fingers—of one phase penetrating the other.

Even in the simplest mathematical framework with only one active phase whose diffusion is modelled by Laplace's equation, and when the interface velocity is proportional to the gradient of the phase, theoretical study of two-dimensional Laplacian growth and its resultant pattern formation involves consideration of difficult nonlinear free boundary problems. One assumption which enables progress is to assume that the fingers are infinitesimally thin and advance at their tips only with velocity proportional to the local gradient of the phase. In terms of complex analysis the fingers can be thought of as evolving slits in the complex plane.

Communicated by Irene Giardina.

✉ N. R. McDonald
n.r.mcdonald@ucl.ac.uk

[1] Department of Mathematics, University College London, Gower Street, London WC1E 6BT, UK

This realisation, coupled with conformal-mapping methods, has resulted in considerable understanding of the Laplacian growth of thin fingers, or their straight-line counterpart: needles e.g. [1,5,17].

Laplace's equation is frequently used as a natural first approximation to more complicated physics when the interface dynamics is governed by a general diffusive-type PDE. Studies concerned with the latter are rare primarily because application of mathematical tools based on complex analytic methods are not immediately obvious for general PDEs. Some exceptions include [11,13,14]. The present work is a contribution to non-Laplacian growth in that it considers Poisson's equation as the governing PDE.

This work considers a specific example of finger growth in a Poisson field (with constant right-hand side) applying to the growth of a stream network incised by groundwater flow. Laplacian growth models have been successful in describing many features of these networks: a prominent example of this being an explanation of the remarkable observation that the angle at which streams bifurcate is close to $2\pi/5$ e.g. [6,7,15]. However, the groundwater flow field ϕ is more appropriately modelled by Poisson's equation, in non-dimensional form, $\Delta\phi = -1$ where the constant right-hand side represents a constant source (precipitation). This paper derives explicit results for fingers growing in a Poisson field which agree with the recent numerical experiments of Cohen and Rothman [4] who grow two or three fingers in a long strip-like channel and find, interestingly, after carrying out a large number of numerical experiments that the fingers eventually grow parallel to the channel boundaries with the same well-defined spacing irrespective of their initial starting locations. Their method and results are discussed in Sect. 2. Here, analytical results using conformal mapping combined with the principle of local symmetry suitably modified to account for the non-zero right hand side of Poisson's equation are derived in Sect. 3 and compared to [4]. The relationship between the Poisson fingers to the analogous Laplacian case is discussed in Sect. 4. The general case of $2N$-fingers is discussed in Sect. 5.

2 Background: The Numerical Experiments of Cohen and Rothman

Cohen and Rothman [4] consider the growth of either 2 or 3 infinitesimally thin fingers in a two-dimensional, narrow strip of width $2l$ and length $L = 50l$. The fingers penetrate the interior of the strip from one of the short sides, and their dynamics determined by solving Poisson's equation $\Delta\phi = -1$, subject to $\phi = 0$ on the fingers and all boundaries of the strip, except the side opposite from which the fingers grow where a zero flux condition $\partial\phi/\partial n = 0$ is imposed. Figure 1 shows the equivalent set-up to be considered here with $l = 1$ and complex coordinates $z = x + iy$ chosen so that the centreline of the strip is aligned with $y = 1$ and the fingers grow from the edge aligned with the imaginary axis $x = 0$, $0 \leq y \leq 2$. The fingers computed in [4] are grown at their tips with constant velocity in directions according to the principle of local symmetry. This involves numerically solving the Poisson equation in the slit domain at a given timestep and using the solution to find the leading terms in the local expansion of $\phi(x, y)$ near the tip of each finger:

$$\phi(r, \theta) = d_1 r^{1/2} \cos(\theta/2) + d_2 r \sin\theta + \mathcal{O}(r^{3/2}), \tag{1}$$

where $d_{1,2}$ are coefficients determined by the global numerical solution of the Poisson problem, r and θ are local polar coordinates such that $\theta = \pm\pi$ coincides with the finger near its tip at $r = 0$. The principle of local symmetry requires that the fingers grows in a direction such that $d_2 = 0$ [3,7]. As noted in [4] while the path selection and growth mechanism of

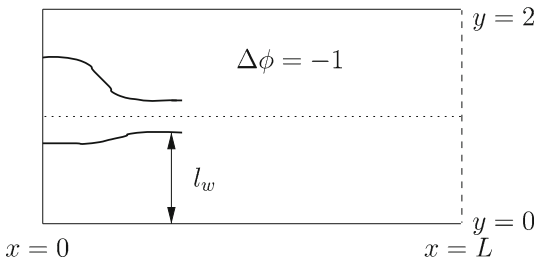

Fig. 1 The strip domain showing finger trajectories (thick curved lines) which asymptotically approach paths parallel to, and distance l_w from, the long boundaries of the strip. The asymptotic paths are equidistant form the centreline of the strip shown by the dotted line. Cohen and Rothman [4] solve Poisson's equation $\Delta\phi = -1$ in the slit domain subject to $\phi = 0$ on all boundaries and fingers, except the dashed line at $x = L$ where a zero flux condition $\partial\phi/\partial x = 0$ is applied. This paper considers the asymptotic problem when the fingers are straight needles parallel to the sides of the strip

fingers is similar at a local level near finger tips for both harmonic (Laplacian) and Poisson fields, the trajectories will differ since the coefficients in (1) depend on the global field.

Using the above procedure Cohen and Rothman [4] carry out a large number of experiments in which they initiate either 2 or 3 fingers at random positions y_i along the edge at $x = 0$ and grow each at constant velocity in directions determined by the principle of local symmetry. Their Fig. 4 shows that after an initial adjustment of order the width of the strip the fingers grow approximately parallel to the long axis of the strip. The notable feature being that irrespective of the starting locations y_i, the fingers asymptotically approach the same particular—selected—paths parallel to the along-strip axis. For 2 fingers, [4] find in 200 numerical experiments with differing initial conditions that the straight paths are symmetrically placed either side of the strip centreline with each finger a distance $l_w = 0.74 \pm 0.027$ from the edge of the strip (see Fig. 1 for the definition of l_w). For 3 fingers, the ultimate selected paths are again symmetric about a middle finger aligned with the strip centreline, with the other two fingers growing parallel at a distance $l_w = 0.60 \pm 0.031$ from the outer edges of strip.

In Sect. 3 the asymptotic length scales l_w are obtained explicitly using conformal mapping combined with the principle of local symmetry suitably modified to account for Poisson's equation.

3 Derivation of Asymptotic Finger Paths

Problem formulation: two finger case Motivated by [4] it is assumed that the selected paths are parallel to the long sides of the strip, are symmetric about the strip centreline and that the fingers themselves are long compared to the strip width, but short compared to the length L of the strip. Thus the problem is approximated by semi-infinite straight fingers in an infinite strip ($L \to \infty$) as shown in the z-plane sketch of Fig. 2. Symmetry about $y = 1$ is assumed so that only half the strip width $0 \le y \le 1$ need be considered. The mathematical task is to find $y_a = l_w$, by solving Poisson's equation in the cut strip, subject to $\phi = 0$ along $y = 0$ and on the finger itself along $y = y_a$, $\phi_y = 0$ along $y = 1$ and $\phi_x = 0$ for $|x| \to \infty$, and that the principle of local symmetry holds at the finger's tip.

Let

$$\phi(x, y) = y - \frac{y^2}{2} + \psi(x, y), \tag{2}$$

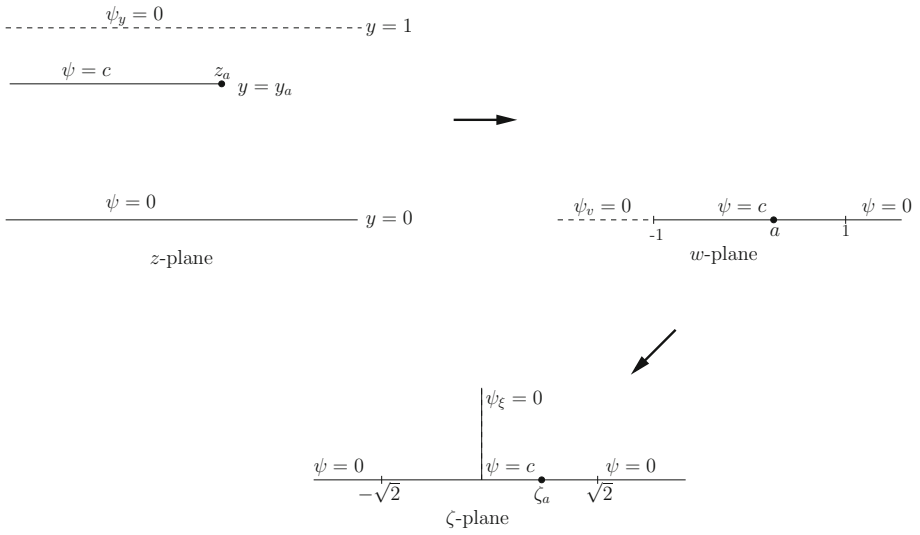

Fig. 2 The sequence of conformal maps from the z to the w-plane and then ζ-plane as indicated by the arrows. The dashed line indicates the portion of the boundary in which the zero flux boundary condition applies. The finger tip z_a is mapped to $w = a$ and then $\zeta = \zeta_a$ with these locations indicated by small dots

so that in the cut strip $\Delta\psi = 0$, and $\psi = 0$ on $y = 0$, $\psi = c = y_a^2/2 - y_a$ on the finger along $y = y_a$, $\psi_y = 0$ on $y = 1$ and $\psi_x = 0$ as $|x| \to \infty$. Since ψ is harmonic, the solution of the boundary problem is facilitated using conformal mapping. The z-plane cut strip geometry is a degenerate polygon and can be mapped to the upper half of the $w = u + iv$ plane by a Schwarz-Christoffel map—see Fig. 2. The map is

$$z = f(w) = \frac{1-a}{2\pi}\log(w-1) + \frac{1+a}{2\pi}\log(w+1), \tag{3}$$

where a is a real parameter such that $|a| < 1$ and maps to the tip of the finger at $z = z_a$ where $y_a = (1-a)/2$ (e.g. [12], p. 155).

The boundary conditions along the real axis of the w-plane are $\psi = c$ for $|u| \le 1$, $\psi = 0$ for $u > 1$, $\psi_v = 0$ for $u < -1$. Additionally, $\nabla\psi \to 0$ for $w \to \infty$. A further map to the ζ-plane given by $\zeta = (1+w)^{1/2}$ maps the upper half of the w-plane to the first quadrant of the ζ-plane, with the zero flux boundary condition being mapped to the positive imaginary axis in the ζ-plane i.e. $\psi_\xi = 0$ on $\xi = 0$, $\eta > 0$, where $\zeta = \xi + i\eta$. This boundary condition implies that it is sufficient to seek a solution to Laplace's equation which is symmetric about the imaginary axis in the upper half of the ζ-plane, with boundary conditions on the real axis $\psi = c$ for $|\xi| \le \sqrt{2}$ and $\psi = 0$ for $|\xi| > \sqrt{2}$. The sequence of maps $z = h(\zeta) = f(w(\zeta))$ is shown in Fig. 2. The image of the finger tip z_a in the ζ-plane is denoted ζ_a.

The solution in the ζ-plane satisfying the zero flux condition at infinity is $\psi = \mathrm{Im}F(\zeta)$ where

$$F(\zeta) = \frac{c}{\pi}\log\left(\frac{\zeta - \sqrt{2}}{\zeta + \sqrt{2}}\right). \tag{4}$$

Principle of local symmetry The principle of local symmetry demands that the behaviour of the ψ field about $z = z_a$ be calculated and so it is necessary to find the first and second derivatives of the map $z = h(\zeta)$ at $\zeta = \zeta_a$. Note

$$h'(\zeta) = \frac{dh}{dw}\frac{dw}{d\zeta} = \frac{2\zeta}{\pi}\frac{w-a}{w^2-1}, \tag{5}$$

and hence that $h'(\zeta_a) = 0$ as expected. Further differentiation yields

$$h''(\zeta_a) = \frac{4\zeta_a^2}{\pi(a^2-1)}, \quad h'''(\zeta_a) = \frac{(5a+3)}{(1-a)}\frac{h''(\zeta_a)}{\zeta_a}. \tag{6}$$

Let $\delta = z - z_a = h(\zeta) - h(\zeta_a)$ be a small displacement that a general point z is from the finger tip z_a, and $\epsilon = \zeta - \zeta_a$ be the corresponding increment in the ζ-plane. Using results in [2] based on Taylor expansion, $\epsilon(\delta)$ can be expanded as series $\epsilon = \alpha_1\delta^{1/2} + \alpha_2\delta + \cdots$ where

$$\alpha_1^2 = \frac{2}{h''(\zeta_a)}, \quad \alpha_2 = -\frac{\alpha_1^2}{6}\frac{h'''(\zeta_a)}{h''(\zeta_a)}. \tag{7}$$

Expanding the difference in complex potential $F(z) - F(z_a) = F(z_a + \epsilon) - F(z_a)$ as a power series in ϵ using solution (4) gives

$$\begin{aligned} F(z) - F(z_a) &= \frac{c}{\pi}\log\left(\frac{\zeta - \sqrt{2}}{\zeta + \sqrt{2}}\right) - \frac{c}{\pi}\log\left(\frac{\zeta_a - \sqrt{2}}{\zeta_a + \sqrt{2}}\right) \\ &= \beta_1\epsilon + \beta_2\epsilon^2 + \mathcal{O}(\epsilon^3) \\ &= \alpha_1\beta_1\delta^{1/2} + (\beta_1\alpha_2 + \beta_2\alpha_1^2)\delta + \mathcal{O}(\delta^{3/2}), \end{aligned} \tag{8}$$

where

$$\beta_1 = \frac{2c\sqrt{2}}{\pi(\zeta_a^2 - 2)}, \quad \beta_2 = -\frac{2c\sqrt{2}\zeta_a}{\pi(\zeta_a^2 - 2)^2}. \tag{9}$$

In the Laplacian case the principle of local symmetry states that the coefficient of δ vanishes in the expansion (8) [3]. Effectively this guarantees that the path taken by the finger is such that it maintains local symmetry in the potential field about the tip and is equivalent to maximising the flux into the tip [4,7]. However in the Poisson case this must be modified owing to the contribution of the term (2) that has been added to ψ needed to satisfy the right hand side of Poisson's equation. In this problem the term is given by $y - y^2/2$. Now, compare (8) with (1) and identify $d_2 = \beta_1\alpha_2 + \beta_2\alpha_1^2$ with the gradient of the potential field (the imaginary part of $F(z)$) near the finger tip in the direction orthogonal to it (here the imaginary i.e. y-direction). In the Poisson case in order that the field be symmetric about the tip this gradient must balance the gradient of the term $y - y^2/2$ in the same direction: $V_a = 1 - y_a$. Thus the principle of local symmetry becomes

$$\beta_1\alpha_2 + \beta_2\alpha_1^2 + V_a = 0. \tag{10}$$

Substituting (6), (7) and (9) into (10) and simplifying gives an algebraic equation for a:

$$(a+3)^2 = \frac{24}{\sqrt{2}}(1+a)^{3/2}, \tag{11}$$

with solution $a \approx -0.48099$ on the permitted interval $|a| \le 1$. This in turn gives $y_a = l_w \approx 0.74$ in agreement with [4] who found $l_w = 0.74 \pm 0.027$.

Three finger case The case of 3 fingers proceeds similarly to the above, the primary difference being the application of different boundary conditions on separate portions of the axis of symmetry $y = 1$ owing to the presence of a growing finger along a semi-infinite part of $y = 1$. It is assumed that this middle finger is of the same length of the other two fingers and

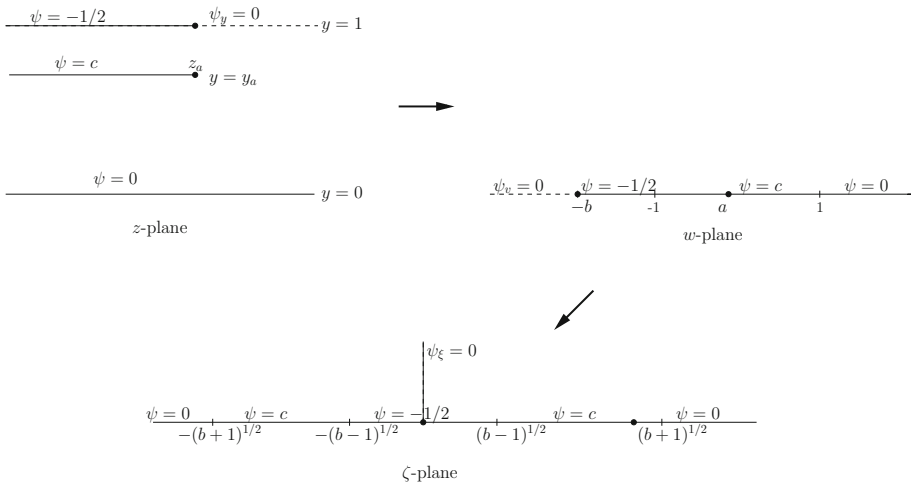

Fig. 3 The sequence of conformal maps for the three finger case from the z to the w-plane and then ζ-plane as indicated by the arrows. The dashed line indicates the portion of the boundary in which the zero flux boundary condition applies. The finger tip z_a is mapped to $w = a$ and then $\zeta = \zeta_a$, while the finger tip along the symmetry axis is mapped to $w = -b$ and then $\zeta = 0$; both are indicated by the small dots

so its tip is at $x_a + i$ while the tip of the other finger in the domain is $x_a + iy_a$. Figure 3 shows the situation. The boundary condition along $y = 1$ is then: $\psi = \phi - y + y^2/2 = -1/2$ along the finger $x \le x_a$, and $\psi_y = 0$ for $x > x_a$. The same conformal map used in the two finger analysis maps the z-plane to the w-plane with $z_b = x_a + i$ being mapped to $w = -b$, where $b > 1$. There are two unknown parameters to be determined: a and b.

In the w-plane the boundary conditions are mapped to the real axis and are $\psi = c$ for $|u| \le 1$; $\psi = 0$ for $u > 1$; $\psi = -1/2$ for $-b \le u < -1$; $\psi_v = 0$ for $u < -b$. Again, the upper half of the w-plane is subsequently mapped to the first quadrant of the ζ-plane via the map $\zeta = (w+b)^{1/2}$ which has the effect of mapping the zero flux boundary condition to the positive imaginary axis in the ζ-plane. Extending the region of consideration to the upper half of the ζ-plane and demanding the solution is symmetric about the imaginary axis results in results in the following boundary conditions along the ξ axis: $\psi = 0$ for $\xi > (b+1)^{1/2}$; $\psi = c$ for $(b-1)^{1/2} < |\xi| < (b+1)^{1/2}$; $\psi = -1/2$ for $|u| < (b-1)^{-1/2}$; and that the gradient of ψ vanishes at infinity—see Fig. 3.

The solution for ψ in the ζ-plane is $\psi = \mathrm{Im}\, f(\zeta)$ where

$$F(\zeta) = \frac{c}{\pi} \log\left(\frac{\zeta - (b+1)^{1/2}}{\zeta + (b+1)^{1/2}}\right) - \frac{(1/2+c)}{\pi} \log\left(\frac{\zeta - (b-1)^{1/2}}{\zeta + (b-1)^{1/2}}\right). \tag{12}$$

Note in this case z_a is mapped successively to $w = a$ and then $\zeta_a = (a+b)^{1/2}$.

Let $z = h(\zeta)$ be the composite map from the ζ-plane to the z-plane. Computing the first three derivatives and evaluating at ζ_a gives as expected $h'(\zeta_a) = 0$, and

$$h''(\zeta_a) = \frac{4\zeta_a^2}{\pi(a^2-1)}, \quad h'''(\zeta_a) = \frac{4\zeta_a}{\pi(a^2-1)^2}(3a^2 - 3 - 8a\zeta_a^2). \tag{13}$$

Expanding the difference in complex potential $F(z)$ (12) evaluated at the points z and z_a as a power series in ϵ of the same form as (8) with now

$$\beta_1 = \frac{(b-1)^{1/2}(1+2c)}{\pi(b-1-\zeta_a^2)} - \frac{2(b+1)^{1/2}c}{\pi(1+b-\zeta_a^2)},$$
$$\beta_2 = \frac{\zeta_a(b-1)^{1/2}(1+2c)}{\pi(b-1-\zeta_a^2)^2} - \frac{2\zeta_a(b+1)^{1/2}c}{\pi(1+b-\zeta_a^2)^2}. \tag{14}$$

In the limit $b \to 1$ (14) reduces to (9); physically in this limit the length of the middle finger becomes negligible compared to the other two fingers and the two finger case is recovered. For the three finger case, the additional unknown parameter b is found by assuming that the length of the middle finger is the same as the two fingers either side, this being consistent with the numerical experiments [4] in which fingers are grown at constant speed. Hence the Schwarz–Christoffel map (3) upon equating real parts for the tips of the fingers gives the following relation between a and b:

$$(1-a)\log(1-a) + (1+a)\log(1+a) = (1-a)\log(b+1) + (1+a)\log(1-b). \tag{15}$$

Substituting (13) into the local symmetry condition (10) gives

$$\pi(5a^2+8ab+3)\beta_1 + 6\pi(a^2-1)\zeta_a\beta_2 = -12\zeta_a^3 V_a, \tag{16}$$

where the coefficients $\beta_{1,2}$ are given by (14). Equations (15) and (16) are a pair of coupled nonlinear equations for a and b which can be solved numerically e.g. using matlab's *vpasolve* routine. The permissible solution is $a \approx -0.2213$ and $b \approx 1.2904$, leading to $y_a = l_w \approx 0.61$ for the three finger case. This is again in good agreement with [4] who find $l_w \approx 0.60 \pm 0.031$.

4 Relation to the Laplacian Growth Case

A similar method to that used in Sect. 3 can be used to find the asymptotic paths selected by fingers growing in a semi-infinite strip which are governed by Laplace's equation $\Delta\phi = 0$. In this case the flux needed to drive the finger growth is provided at infinity. Paths can be found using two alternative methods: the first methods proceeds by solving the chordal Loewner equation for slit evolution in the upper half of the w-plane and then mapping the paths to the strip domain. This is done below and then the result compared to that using the method used in Sect. 3.

The Laplacian paths which obey the principle of local symmetry ('geodesic' Loewner paths) for two fingers growing from the real axis into the upper half ζ^*-plane while maintaining symmetry about the imaginary axis are known exactly [9]. After initial adjustment they approach straight line paths diverging with an angle $\pi/5$ between them. That is, fingers, on which $\phi = 0$, asymptote toward the rays $r\exp(2\pi/5)$ and $r\exp(3\pi/5)$ where r and θ are polar coordinates with $\theta = 0, \pi$ coinciding with the real w-axis along which $\phi = 0$. The far-field condition used in deriving the solution is that used in standard Loewner growth: $\phi \to \mathrm{Im}(\zeta^*)$ as $\zeta^* \to \infty$.

To find the equivalent paths in a semi-infinite strip (the z-plane) with $\phi = 0$ on all boundaries, the above finger trajectories (assumed to emanate from the interval $|\mathrm{Re}w| \le 1$) are simply mapped to the z-plane using the map $\zeta^* = \cosh(\pi z/2)$ which takes the upper half of the ζ^*-plane to the semi-infinite strip $0 \le y \le 2$ and $x > 0$. Interest here is on the far-field paths, one branch of which tends to

$$x + iy = \frac{2}{\pi}\cosh^{-1}\left(re^{2\pi i/5}\right), \quad \text{as} \quad r \to \infty. \tag{17}$$

and so $y \to 4/5$, a path a distance 0.2 from the centreline $y = 1$. The other path is symmetrically placed the other side of the strip centreline.

The method of Sect. 3 is now used to reproduce this result: two fingers are assumed to grow parallel and equidistant from the strip centreline as in Fig. 2. The condition $\psi = c$ is replaced by $\psi = 0$ in the Laplacian case since there is no difference between ϕ and ψ. The primary difference is instead of the vanishing flux condition at infinity used in Sect 2, the far-field condition in the z-plane is now $\phi \to \text{Im}[\frac{1}{2}\exp(\pi z/2)]$. This condition comes from the map $\zeta^* = \cosh(\pi z/2)$ applied to the standard chordal Loewner far-field condition $\phi \to \text{Im}\zeta^*$ as $\zeta^* \to \infty$.

After the same successive transformations from the z to w and then ζ-planes described in Sect 3, the problem in the ζ-plane then becomes that of finding a harmonic field ψ which vanishes on the real axis. Note that in this sequence of transformations the far-field behaves as $z \to (1/\pi)\log w \to (2/\pi)\log\zeta$. Hence in the ζ-plane, ψ tends to $(1/2)\text{Im}\zeta$ at infinity, and thus $\psi = \text{Im}F(z)$ where $F(z) = \zeta/2$ is the solution. Expanding $F(z) - F(z_a)$ in the same way as (8) gives $\beta_1 = 1/2$ and $\beta_2 = 0$, for which in turn the principle of local symmetry (10) with $V = 0$ immediately gives $a = -3/5$ or $y_a = l_w = 4/5$. Essentially this symmetry principle is equivalent to demanding that the third derivative (6) $h'''(\zeta_a) = 0$—see also [2]). The fingers grow parallel and distance 0.2 either side of the centreline in agreement to the above argument based on mapping the solution [9] for 2 fingers growing in the half-plane.

5 General Case: 2*N* Fingers

This section generalises the method of Sect. 3 to determine the paths selected by $2N$ parallel fingers propagating along the strip i.e. N fingers placed symmetrically either side of the centreline. It is possible to also consider the $2N + 1$ finger case with the middle finger propagating along the centreline but the details are not presented here.

Let $z_i = x_i + iy_i$, $i = 1, \ldots, N$ be the tips of the N fingers arranged with increasing imaginary part i.e. $0 < y_1 < \cdots < y_N < 1$. It is assumed that the fingers are of equal length: $x_i = x_j$ for all i and j. On each finger $\psi = c_i = y_i^2/2 - y_i$ and, as before, $\psi = 0$ on $y = 0$ and $\psi_y = 0$ on the centreline $y = 1$.

The Schwarz–Christoffel map from the upper half of the w-plane to the z-plane $z = f(w)$ can be constructed from the primitive

$$\frac{df}{dw} = \frac{1}{\pi}\frac{(w-a_1)(w-a_2)\cdots(w-a_N)}{(w-1)(w-b_2)\cdots(w-b_N)(w+1)}, \tag{18}$$

where $w = a_i$, $i = 1, \ldots, N$, are real parameters such that $z_i = f(a_i)$, and b_i are real parameters which map to $x \to -\infty$. The parameters are ordered according $a_i > b_{i+1} > a_{i+i}$, $i = 1, N-1$. Figure 4 shows the finger arrangement in the z-plane and the sequence of a_i and b_i on the real w-axis. Further, define $b_1 = 1$ and $b_{N+1} = -1$. The parameters a_i, $i = 1, \ldots, N$ and b_i, $i = 2, \ldots, N$ represent $2N - 1$ unknown real parameters which need to be found.

Writing (18) as partial fractions and integrating gives $z = f(w)$

$$z = \frac{1}{\pi}\sum_{i=1}^{N+1}\gamma_i \log(w - b_i), \tag{19}$$

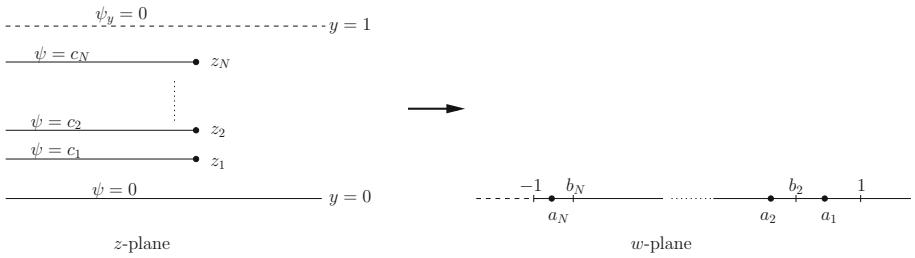

Fig. 4 Conformal map from the z-plane to the w-plane for N slits. The finger tips $z_1, \ldots, z_N$ map to $a_1, \ldots, a_N$. The points $b_1, \ldots, b_N$ represent the images of the points at infinity between the slits. The zero normal flux condition hold on the dashed lines

where γ_i are real constants determined from the a_j and b_j by

$$\gamma_i = \frac{\prod_{j=1}^{N}(b_i - a_j)}{\prod_{\substack{j=1 \\ (j\neq i)}}^{N+1}(b_i - b_j)}, \quad i = 1, \ldots, N+1. \tag{20}$$

The distances y_i of the fingers from the strip boundary $y = 0$ are found by considering the imaginary part of the logarithms in (19)

$$y_i = \sum_{j=1}^{i} \gamma_j, \quad i = 1, \ldots, N. \tag{21}$$

Demanding that all N fingers have the same length gives $N - 1$ equations of the form $x_1 = x_2$, $x_1 = x_3$ etc., where

$$\pi x_i = \sum_{j=1}^{N+1} \gamma_j \log|a_i - b_j|. \quad i = 1, \ldots, N. \tag{22}$$

A further N equations for the unknown parameters are obtained by considering the principle of local symmetry at each of the N finger tips. As in Sect. 3, the upper half of the w-plane is mapped via a square root $\zeta = (w+1)^{1/2}$ to the first quadrant on the ζ-plane which is subsequently extended to the entire upper half ζ-plane by virtue of the symmetry condition along the imaginary ζ-axis. The complex potential in the ζ-plane is then

$$F(z) = \frac{1}{\pi}\sum_{j=1}^{N}(c_j - c_{j-1}) \log\left(\frac{\zeta - (b_j+1)^{1/2}}{\zeta + (b_j+1)^{1/2}}\right), \tag{23}$$

where $c_0 = 0$ is understood.

Now considering the principle of local symmetry at each tip requires calculation of the expansion $F(\zeta_{a_i} + \epsilon) - F(\zeta_{a_i}) = \beta_{1i}\epsilon + \beta_{2i}\epsilon^2 \cdots = d_{1i}\delta^{1/2} + d_{2i}\delta + \cdots$, where $\beta_{1i}\alpha_{2i} + \beta_{2i}\alpha_{1i}^2 = d_{2i}$. The first two terms in the expansion of $F(z_{a_i} + \epsilon) - F(z_{a_i})$ using (23) are

$$\begin{aligned} \beta_{1i} &= \frac{2}{\pi}\sum_{j=1}^{N}\frac{(c_j - c_{j-1})(b_j+1)^{1/2}}{\zeta_{a_i}^2 - b_j - 1} \\ \beta_{2i} &= -\frac{2}{\pi}\sum_{j=1}^{N}\frac{(c_j - c_{j-1})(b_j+1)^{1/2}\zeta_{a_i}}{(\zeta_{a_i}^2 - b_j - 1)^2}, \end{aligned} \tag{24}$$

and the coefficients α_{1i} and α_{2i} have the same form as (7) and are calculated from the map (19).

Once the expressions d_{2i} are found then local symmetry demands

$$d_{2i} + V_i = 0, \quad i = 1, \ldots, N, \tag{25}$$

where $V_i = 1 - y_i = 1 - \sum_{j=1}^{i} \gamma_i$. Thus (25) together with the $N-1$ equal length conditions give $2N-1$ equations for the $2N-1$ unknown parameters a_i and b_i.

Example: $N = 4$ Solving (e.g. using matlab routine *vpasolve*) the three nonlinear coupled equations $x_1 = x_2$ given by (22) and (25) for $i = 1, 2$ for the unknown parameters a_1, a_2 and b_1 on the interval $[-1, 1]$ gives

$$a_1 \approx 0.1816, \quad a_2 \approx -0.8578, \quad b_1 \approx -0.4341, \tag{26}$$

which in turn from (20) and (21) determines the elevation of each of the fingers: $y_1 \approx 0.53$ and $y_2 \approx 0.85$.

6 Concluding Remarks

Explicit solutions for the asymptotic paths selected by fingers in a Poisson field have been found which compare well with the equivalent paths recently found numerically [4]. The method relies on finding a particular solution for the Poisson field, and then using conformal mapping on the resulting harmonic problem to find the local field in the vicinity of the fingertips. The principle of local symmetry, suitably modified to account for the particular solution needed to account for the Poisson forcing, determines the unknown parameters of the mapping enabling the paths selected by the fingers to be calculated. To the author's knowledge these are the first exact solutions, albeit applying to the asymptotic idealisation to the finite length strip geometry, for the non-Laplacian growth of infinitesimally thin fingers.

It is of interest to see if a similar approach can be usefully employed in other geometries and boundary conditions, and for other forms of Poisson forcing which may involve either non-constant or time varying functions. Beyond Poisson's equation, other elliptic PDEs are relevant to modelling other physical processes and studying their fingering patterns is also of interest e.g. stream networks formed by the non-Laplacian flow of groundwater with spatially varying diffusivity.

While the fingers here evolve steadily in a fixed direction, the time-varying problem in which they take curved paths requires study. The classical approach to studying slit evolution in the half-plane involves solution of the chordal Loewner equation. In Laplacian growth this involves so-called geodesic dynamics [1,7,9,17] in which the Loewner forcing function has a precise form and results in paths equivalent to those which evolve according to the principle of local symmetry [7]. How is this Loewner evolution modified for Poisson growth? Even more fundamentally, it is interesting to speculate on whether it is possible to derive a Loewner-type equation governing slit evolution in a Poisson field. The approach taken here of finding a particular solution for the inhomogeneous Poisson term results in a harmonic problem for the potential ψ to be solved subject to $\psi \neq 0$ on the fingers. Approximating the fingers as straight needles evolving parallel to the strip meant here that $\psi = constant$ on the fingers, but in general, $\psi = \psi_0(x, y)$ on curved fingers where ψ_0 is a given function depending on the choice of particular solution. It is an open problem to incorporate boundary conditions more general than $\psi = 0$ on fingers in Loewner theory.

Another approximation employed here which does not necessarily apply in more realistic scenarios is the assumption that the different fingers grow with the same velocity. In contrast, it is well-known that interacting fingers and needles grow competitively with velocities proportional to the local gradient of the phase field at their tips [1,5], with the effect that longer fingers tend to grow more rapidly than shorter fingers. This effect, referred to as screening, plays a key role in determining patterns selected in finger growth [1,5,9].

Section 4 shows the paths selected by Laplacian fingers are different to those than in the Poisson case. There is no continuous parameter which connects the two limits since the forcing is different: in the Laplacian case there is a flux from infinity, whereas in the Poisson case the forcing is uniform over the whole domain. However, by combining the two different forcings in an appropriate proportion related to the constant on the RHS of the Poisson equation is may be possible to connect them continuously, though this set-up is perhaps physically difficult to justify. From the stream network development view, use of the Laplace approximation has been highly successful in explaining phenomenon which act on a local level (e.g. stream bifurcation), but the same approximation should be used with caution over larger scales when streams interact with each other and far-field boundary conditions.

Acknowledgements I am grateful for helpful discussion with Dan Rothman and Eric Stansifer during a visit to MIT funded by a UCL Global Engagement grant. The reviewers made useful comments.

References

1. Carleson, L., Makarov, N.: Laplacian path models. J. d'Analyse Math. **87**(1), 103–150 (2002)
2. Cohen, Y., Devauchelle, O., Seybold, H.F., Yi, R.S., Szymczak, P., Rothman, D.H.: Where do rivers grow? Path selection in a harmonic field. arXiv:1409.8140 [physics.geo-ph] (2014)
3. Cohen, Y., Devauchelle, O., Seybold, H.F., Yi, R.S., Szymczak, P., Rothman, D.H.: Path selection in the growth of rivers. Proc. Natl. Acad. Sci. **112**(46), 14132–14137 (2015)
4. Cohen, Y., Rothman, D.H.: Path selection in a Poisson field. J. Stat. Phys. **167**, 703–712 (2017)
5. Derrida, B., Hakim, V.: Needle models of Laplacian growth. Phys. Rev. A **45**, 8759–8765 (1992)
6. Devauchelle, O., Petroff, A.P., Seybold, H.F., Rothman, D.H.: Ramification of stream networks. Proc. Natl. Acad. Sci. **109**(51), 20832–20836 (2012)
7. Devauchelle, O., Szymczak, P., Pecelerowicz, M., Cohen, Y., Seybold, H.J., Rothman, D.H.: Laplacian networks: growth, local symmetry, and shape optimization. Phys. Rev. E **95**, 033113 (2017)
8. Giverso, C., Verani, M., Ciarletta, P.: Branching instability in expanding bacterial colonies. J. R. Soc. Interface **12**, 20141290 (2015)
9. Gubiec, T., Szymczak, P.: Fingered growth in channel geometry: a Loewner-equation approach. Phys. Rev. E **77**, 041602 (2008)
10. Johansen, T.H., Baziljevich, M., Shantsev, D.V., Goa, P.E., Galperin, Y.M., Kang, W.N., Kim, H.J., Choi, E.M., Kim, M.S., Lee, S.I.: Dendritic magnetic instability in superconducting MgB_2 films. Europhys. Lett. **59**(4), 599–605 (2002)
11. Khavinson, D., Mineev-Weinstein, M., Putinar, M.: Planar elliptic growth. Complex Anal. Oper. Theor. **3**(2), 425–451 (2009)
12. Kober, H.: Dictionary of Conformal Representations, 2nd edn. Dover, New York (1957)
13. Lundberg, E.: Laplacian growth, elliptic growth, and singularities of the Schwarz potential. J. Phys. A **44**, 135202 (2011)
14. McDonald, N.R., Mineev-Weinstein, M.: Poisson growth. Anal. Math. Phys. **5**(2), 193–205 (2015)
15. Petroff, A.P., Devauchelle, O., Seybold, H., Rothman, D.H.: Bifurcation dynamics of natural drainage networks. Philos. Trans. Soc. A **371**, 20120365 (2013)

16. Saffman, P., Taylor, G.: The penetration of a fluid into a porous medium or Hele-Shaw cell containing a more viscous liquid. Proc. R. Soc. Lond. A **245**(4), 312–329 (1958)
17. Selander, G.: Two deterministic growth models related to diffusion-limted aggregation. Ph.D. thesis, Royal Inst. Tech., Stockholm (1999)
18. Witten, T.A., Sander, L.M.: Diffusion-limited aggregation, a kinetic critical phenomenon. Phys. Rev. Lett. **47**, 1400–1403 (1981)
19. Zik, O., Olami, Z., Moses, E.: Fingering instability in combustion. Phys. Rev. Lett. **81**, 3868–3871 (1998)